

Oxidative thermolysis of $\text{Mn}(\text{acac})_3$ on the surface of γ -alumina support

Igor V. Babich^{a,1}, Lyudmyla A. Davydenko^{a,*}, Lyudmila F. Sharanda^a,
Yuri V. Plyuto^a, Michiel Makkee^b, Jacob A. Moulijn^b

^a Institute of Surface Chemistry, National Academy of Sciences of Ukraine, General Naumov Str. 17, 03164 Kiev, Ukraine

^b DelfChemTech, Delft University of Technology, Julianalaan 136, 2628 BL Delft, The Netherlands

Received 16 July 2006; received in revised form 10 February 2007; accepted 15 February 2007

Available online 24 February 2007

Abstract

Precipitated γ -alumina support was decorated with $\text{Mn}(\text{acac})_3$ by incipient wetness impregnation with toluene solutions containing $\text{Mn}(\text{acac})_3$ in amount equivalent to loading of 0.35, 0.74, 1.38, 2.38 and 3.50 $\text{Mn}(\text{acac})_3$ molecules per nm^2 of the support. In order to evaluate the mechanism of $\text{Mn}(\text{acac})_3$ interaction with the surface of γ -alumina support and subsequent transformations of the supported $\text{Mn}(\text{acac})_3$ species, oxidative thermolysis of $\text{Mn}(\text{acac})_3/\text{Al}_2\text{O}_3$ samples in air was studied by diffuse reflectance FTIR, thermogravimetric analysis (TG/DTG), differential thermal analysis (DTA) and XRD. It has been found out that decoration of $\gamma\text{-Al}_2\text{O}_3$ support with $\text{Mn}(\text{acac})_3$ results in the formation of surface bound $\text{Mn}(\text{acac})_{3-x}$ species when $\text{Mn}(\text{acac})_3$ loading does not exceed 1.38 $\text{Mn}(\text{acac})_3/\text{nm}^2$. At higher $\text{Mn}(\text{acac})_3$ loading the formation of the supported bulk-like $\text{Mn}(\text{acac})_3$ species also occurs. The interaction of $\text{Mn}(\text{acac})_3$ molecules with the support surface occurs via substitution of acetylacetonate ligand(s) with the oxygen atom of surface hydroxyl group(s) accompanied by elimination of acetylacetone molecules. The evolved acetylacetone reacts with the alumina surface that results in the formation of surface $\text{Al}(\text{acac})_{3-x}$ species. The oxidative thermolysis of $\text{Mn}(\text{acac})_{3-x}$ species on the surface of γ -alumina proceeds via partial elimination of acetylacetonate ligands and partial oxidation of the remaining ligands without destruction of their cyclic structure within 425–550 K. The complete oxidative destruction of acetylacetonate ligands takes place within 600–700 K and results in the formation of manganese oxide species on the alumina surface. The dispersed surface manganese oxide species originate upon the oxidative thermolysis of the surface bound $\text{Mn}(\text{acac})_{3-x}$ species while crystalline Mn_2O_3 phase results from the supported bulk-like $\text{Mn}(\text{acac})_3$ species.

© 2007 Elsevier B.V. All rights reserved.

Keywords: γ -alumina; $\text{Mn}(\text{acac})_3$; Thermolysis

1. Introduction

Application of metal β -diketonates for processing of supported catalysts is of great interest because of possibility to control precisely the dispersion of supported active phase. Metal acetylacetonates, in particular, are stated to be promising precursor of heterogeneous catalysts [1,2]. Volatility of some acetylacetonates ($\text{Cr}(\text{acac})_3$, $\text{Al}(\text{acac})_3$, $\text{V}(\text{acac})_3$, $\text{Pt}(\text{acac})_2$ or $\text{Cu}(\text{acac})_2$) makes possible their vapour phase deposition onto support surface. Thermally unstable acetylacetonates ($\text{Co}(\text{acac})_2$, $\text{Fe}(\text{acac})_3$ or $\text{Mn}(\text{acac})_3$) can be deposited by

adsorption from organic solvents. High dispersion degree of supported metal acetylacetonates is achievable due to their H-bonding with surface groups of support or ligand substitution [2,3]. Oxidative thermolysis of metal acetylacetonates is accompanied with formation of environmentally benign by-products (carbon dioxide and water). Mild conditions of ligand elimination prevent sintering of the supported phase. Studies of thermal activation of supported $\text{VO}(\text{acac})_2$ [3], $\text{Cr}(\text{acac})_3$ [4], $\text{MoO}_2(\text{acac})_2$ [5], $\text{Co}(\text{acac})_3$ [6], $\text{Co}(\text{acac})_2$ [6,7] and $\text{Ni}(\text{acac})_2$ [8,9] in order to prepare heterogeneous catalysts of well-defined structure were recently undertaken.

Supported manganese oxides are known to be suitable catalysts for numerous processes, i.e. ozonation [10], decomposition [11] and oxidation [12–16]. Catalytic activity correlates with dispersion of active phase [10,13]. High dispersion of supported manganese oxide should be achieved for preparing efficient catalyst. The precursor of active phase has a great influence on

* Corresponding author. Tel.: +38 44 422 9653; fax: +38 44 424 3567.

E-mail address: l.davydenko@yahoo.com (L.A. Davydenko).

¹ Present address: Catalytic Processes and Materials, Faculty of Science and Technology, IMPACT, University of Twente, P.O. Box 217, 7500AE Enschede, The Netherlands.

its dispersion [17]. Taking into consideration the advantages of metal acetylacetonates, we suppose manganese acetylacetonate to be suitable precursor for preparation of highly dispersed alumina supported manganese oxide. Despite great interest in metal acetylacetonates and supported manganese oxides, the synthesis of heterogeneous manganese-based catalysts via $\text{Mn}(\text{acac})_x$ ($x=2$ or 3) precursor has not widely realized. Only several researches concern the use of $\text{Mn}(\text{acac})_2$ for catalyst preparation [18,19].

Present work was aimed at studies of $\text{Mn}(\text{acac})_3$ interaction with the surface of γ -alumina support and subsequent transformations of the supported $\text{Mn}(\text{acac})_3$ species upon oxidative thermolysis.

2. Experimental

The pelleted γ - Al_2O_3 (CK 300, Ketjen, $S_{\text{BET}}=250\text{ m}^2/\text{g}$) was first crushed to a particle size of 0.25–0.50 mm and calcined at 773 K for 2 h in air just before impregnation. Toluene and $\text{Mn}(\text{acac})_3$ were obtained from Aldrich and used without further purification. The impregnation solutions were prepared by dissolving appropriate amount of $\text{Mn}(\text{acac})_3$ in the volume of toluene which corresponds to the pore volume of γ -alumina support. Decoration of γ -alumina supports with $\text{Mn}(\text{acac})_3$ were done by incipient wetness impregnation using its toluene solution followed by the samples drying at 373 K for 2 h in air. Because of the limited solubility of $\text{Mn}(\text{acac})_3$ in toluene, the samples were prepared either by single or multiple impregnation-drying. The samples with manganese loading of 0.35, 0.74, 1.38 $\text{Mn}(\text{acac})_3/\text{nm}^2$ (0.8, 1.6 and 3.0 Mn wt% in the calcined samples) were synthesised using a single impregnation-drying procedure. The samples with manganese loading of 2.38 and 3.50 $\text{Mn}(\text{acac})_3/\text{nm}^2$ (5.0 and 7.0 Mn wt% in the calcined samples) were prepared by two- and three-fold repetition of impregnation-drying procedures, respectively.

The total manganese content in the synthesised samples was determined by flame atomic absorption spectroscopy after their calcination at 873 K for 3 h in air and subsequent dissolving. A portion of approximately 20 mg of a sample was placed in a conic flask and 5 cm^3 of concentrated sulphuric acid was added. Then the flask was heated to a temperature essential for observation of a slight fume at its exit and kept at this temperature for 5 h. After cooling, approximately 20 cm^3 of demineralised water and 1–2 drops of 30% aqueous solution of hydrogen peroxide were added. Then the mixture was boiled until it became clear. The resulting solution was transferred into calibrated flask and adjusted to 50 cm^3 with demineralised water.

Diffuse reflectance FTIR spectra were recorded with a Magna-IRTM-550 spectrometer equipped with a reflectance cell in the range of 950–1900 cm^{-1} with resolution 2 cm^{-1} . The samples were diluted with KBr (1:10), finely ground and mounted in a microcup. The spectra were normalised against the KBr background and presented in Kubelka–Munk units.

Thermogravimetric analysis (TG/DTG) and simultaneous differential thermal analysis (SDTA) were carried out with a Mettler-Toledo TGA/SDTA851^e thermobalance at a heating rate of 10 K/min in air flow of 100 cm^3/min .

XRD analysis of the calcined samples was performed with a Philips PW 1840 diffractometer using Cu K α radiation.

3. Results and discussion

The decorated γ -alumina supports with 0.35, 0.74, 1.38, 2.38 and 3.50 $\text{Mn}(\text{acac})_3/\text{nm}^2$ loading, denoted hereinafter as $\text{Mn}(\text{acac})_3/\text{Al}_2\text{O}_3$ samples, were characterised by diffuse reflectance FTIR in order to clarify the mechanism of $\text{Mn}(\text{acac})_3$ interaction with the alumina surface. The absorption bands within the region of 1700–1000 cm^{-1} were observed in IR spectra of all $\text{Mn}(\text{acac})_3/\text{Al}_2\text{O}_3$ samples (Fig. 1). These bands are characteristic for acetylacetonate ligands [20,21]. The spectrum of γ -alumina support modified with acetylacetonate ($\text{Hacac}/\text{Al}_2\text{O}_3$ sample) as well as that of bulk $\text{Mn}(\text{acac})_3$ are also shown in Fig. 1 for comparison.

Two groups of $\text{Mn}(\text{acac})_3/\text{Al}_2\text{O}_3$ samples can be distinguished depending on the character of their IR spectra (Fig. 1). One can see that IR spectra of the $\text{Mn}(\text{acac})_3/\text{Al}_2\text{O}_3$ samples with 0.35, 0.74 and 1.38 $\text{Mn}(\text{acac})_3/\text{nm}^2$ loading exhibit the bands at 1536, 1463, 1403 and 1294 cm^{-1} . These bands are also observed in IR spectrum of $\text{Hacac}/\text{Al}_2\text{O}_3$ sample and are typical for acetylacetonate coordinated to Al^{3+} [22–24]. With increasing of $\text{Mn}(\text{acac})_3$ loading in the samples, the contribution of bands at 1420 and 1387 cm^{-1} into the spectrum gets more valuable. These bands are typical for $\text{Mn}(\text{acac})_3$ [20]. It is clear that acetylacetonate ligands coordinated to Al^{3+} as well as to Mn^{3+} are present in the $\text{Mn}(\text{acac})_3/\text{Al}_2\text{O}_3$ samples that can be evidence of

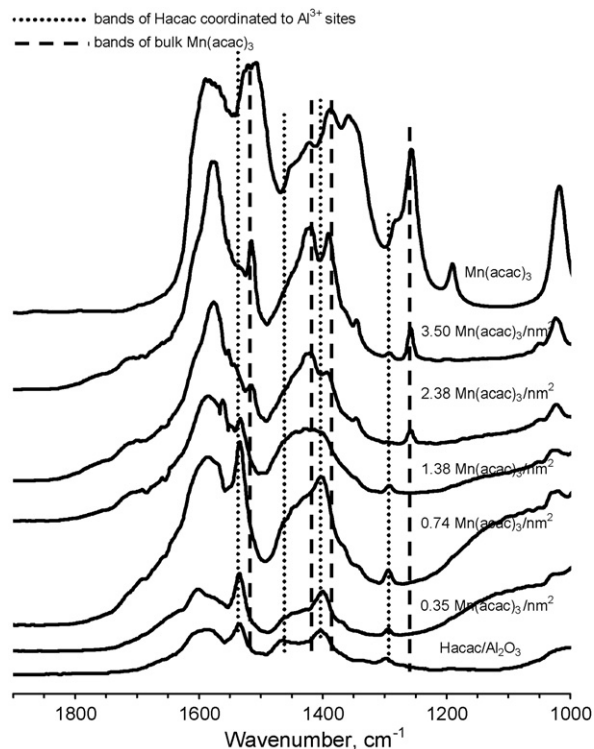
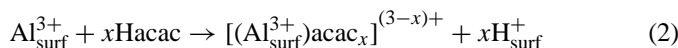
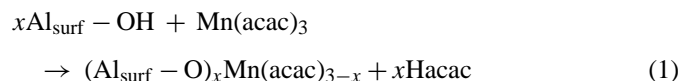


Fig. 1. FTIR spectra of bulk $\text{Mn}(\text{acac})_3$, $\text{Hacac}/\text{Al}_2\text{O}_3$ sample and $\text{Mn}(\text{acac})_3/\text{Al}_2\text{O}_3$ samples with different $\text{Mn}(\text{acac})_3$ loading.

following transformations:



In contrast, IR spectra of $\text{Mn}(\text{acac})_3/\text{Al}_2\text{O}_3$ samples with 2.38 and 3.5 $\text{Mn}(\text{acac})_3/\text{nm}^2$ loading (Fig. 1) possess the clear bands at 1515, 1420, 1387 and 1254 cm^{-1} which are characteristic for bulk $\text{Mn}(\text{acac})_3$. The intensity of the bands at 1536, 1463, 1403 and 1294 cm^{-1} of acetylacetonate species coordinated to Al^{3+} is negligible in contrast to the samples with 0.35, 0.74 and $1.38\text{ Mn}(\text{acac})_3/\text{nm}^2$ loading. These spectral changes occur when $\text{Mn}(\text{acac})_3$ loading exceeds $1.38\text{ Mn}(\text{acac})_3/\text{nm}^2$. One can conclude about the surface bound $\text{Mn}(\text{acac})_{3-x}$ species below $1.38\text{ Mn}(\text{acac})_3/\text{nm}^2$ loading and the presence of supported bulk-like $\text{Mn}(\text{acac})_3$ species above this limit.

The results of IR characterisation of $\text{Mn}(\text{acac})_3/\text{Al}_2\text{O}_3$ samples with different $\text{Mn}(\text{acac})_3$ loading makes it possible to propose the mechanism of structural transformations of $\text{Mn}(\text{acac})_3$ upon deposition on the surface of γ -alumina support. The interaction of $\text{Mn}(\text{acac})_3$ molecules with the support surface occurs via substitution of acetylacetonate ligand(s) with the oxygen atom of surface hydroxyl group(s). This results in the formation of surface bound $\text{Mn}(\text{acac})_{3-x}$ species and elimination of the molecules of acetylacetonate, Hacac. The evolved acetylacetonate reacts with the coordinatively unsaturated Al^{3+} sites of the alumina surface.

The influence of the alumina surface on the process of oxidative thermolysis of the supported $\text{Mn}(\text{acac})_3$ species was studied by IR spectroscopy and thermal analysis.

In order to do this, the thermal decomposition of bulk $\text{Mn}(\text{acac})_3$ was studied in detail. One can see that the thermolysis of bulk $\text{Mn}(\text{acac})_3$ in air proceeds in three steps (Fig. 2a).

The first distinct 20% weight loss occurs at 450 K and is accompanied with slight exothermal effect. One can suppose that it should be attributed to the transformation of $\text{Mn}(\text{acac})_3$ to $\text{Mn}(\text{acac})_2$ via homolytic scission of one acetylacetonate ligand [25]. However, the observed 20% weight loss is substantially less than theoretically expected 28% one for the removal of one acetylacetonate ligand and has to be explained. Besides, the changes in IR spectra of bulk $\text{Mn}(\text{acac})_3$ (Fig. 2b) which are observed upon thermal treatment from 300 to 473 K cannot be ascribed only to removal of acetylacetonate ligand. The relative intensity of the bands at 1356 and 1387 cm^{-1} , characteristic for $-\text{CH}_3$ groups, decreases if compared with the bands at 1420 and 1450 cm^{-1} , characteristic for the compounds which contain the methylene group with active hydrogen ($-\text{CH}_2-\text{CO}-$). Such spectral changes cannot be observed upon only homolytic scission of the acetylacetonate ligand from $\text{Mn}(\text{acac})_3$ molecule. Furthermore, the low-intense bands at 1296 cm^{-1} (C–H in $-\text{CHO}$) and 1660 – 1745 cm^{-1} (C=O in $-\text{CHO}$, $-\text{CO}-$ and $-\text{COO}^-$) appeared in IR spectrum. This can be explained by the partial oxidation of acetylacetonate ligands, namely $-\text{CH}_3$ group into $-\text{CHO}$ group. The process of elimination of one acetylacetonate ligand accompanied with oxidation of one $-\text{CH}_3$ group to $-\text{CHO}$ in the

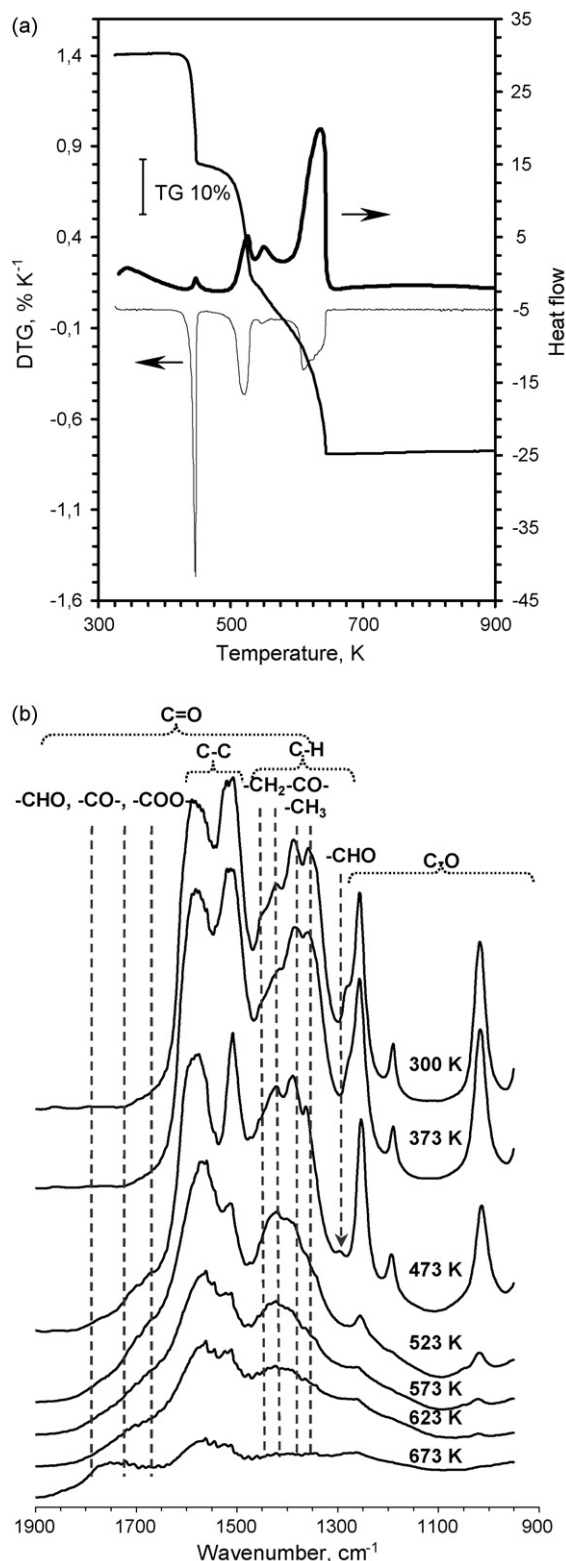


Fig. 2. Thermal decomposition of bulk $\text{Mn}(\text{acac})_3$: (a) TG, DTG and SDTA curves and (b) FTIR spectra of bulk $\text{Mn}(\text{acac})_3$ after thermal treatment at different temperatures.

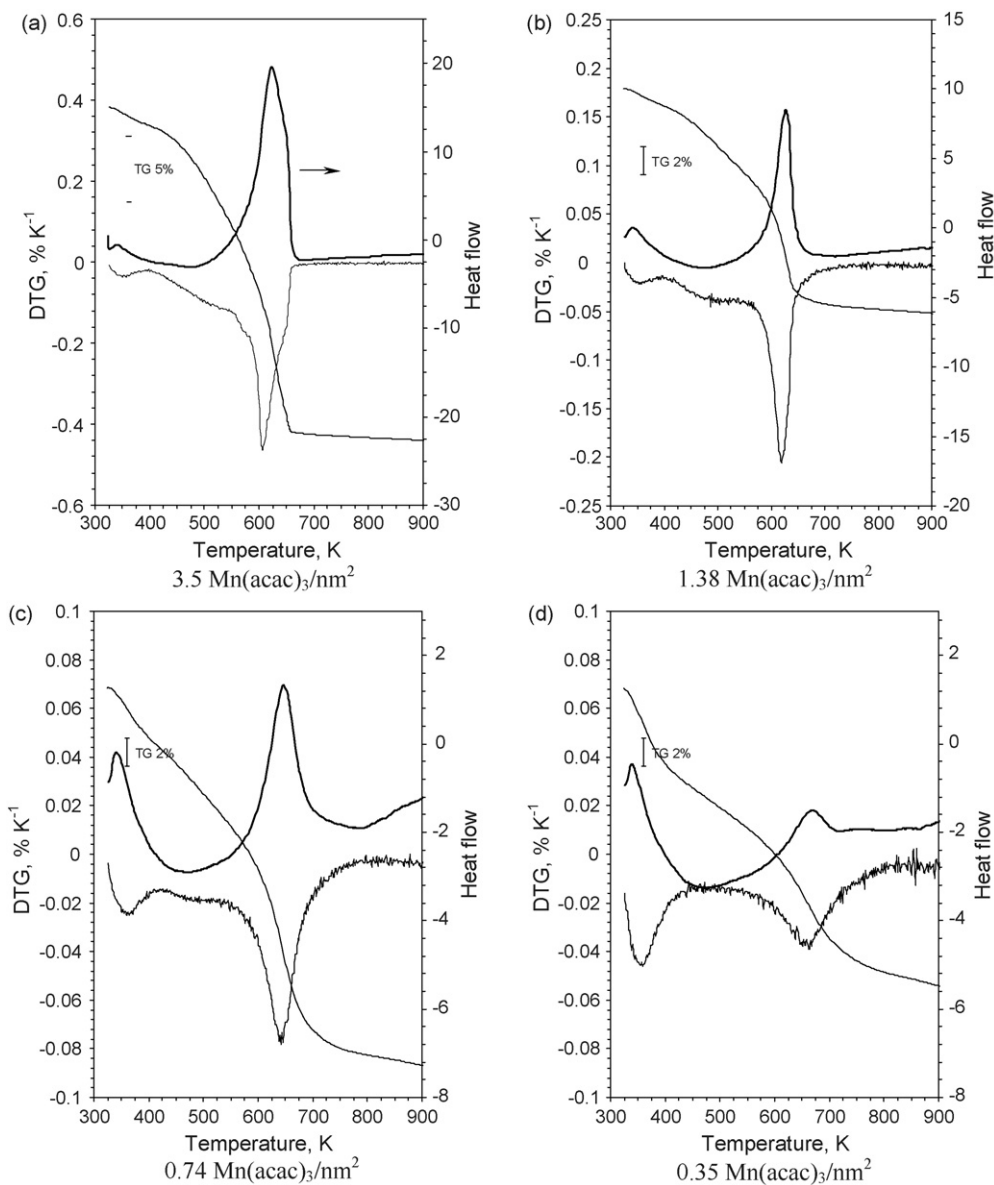
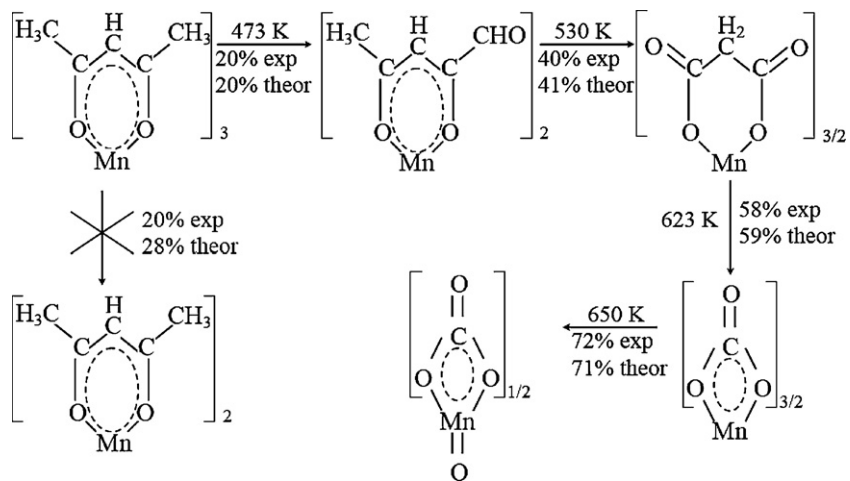


Fig. 3. Thermal decomposition of $\text{Mn}(\text{acac})_3/\text{Al}_2\text{O}_3$ samples with $\text{Mn}(\text{acac})_3$ loading of: (a) $3.5 \text{ Mn}(\text{acac})_3/\text{nm}^2$; (b) $1.38 \text{ Mn}(\text{acac})_3/\text{nm}^2$; (c) $0.74 \text{ Mn}(\text{acac})_3/\text{nm}^2$ and (d) $0.35 \text{ Mn}(\text{acac})_3/\text{nm}^2$.

remaining acetylacetonate ligands (Scheme 1) should result in theoretically calculated 20% weight loss and is in good agreement with experimentally observed value at 473 K.

The second weight loss within 500–530 K (Fig. 2a) is accompanied with exothermic effect and substantial changes in IR spectra (Fig. 2b). The intensity of the bands at 1356 and 1387 cm^{-1} (C–H) and 1506 cm^{-1} (C=C) decreases substantially. The observed 41% weight loss at 500–530 K almost coincides with the theoretically calculated value which corresponds to total oxidation of $-\text{CH}_3$ groups and oxidation of Mn^{2+} to Mn^{3+} (Scheme 1).

The third weight loss within 600–650 K (Fig. 2a) is accompanied with a substantial exothermic effect. The weight loss peak is broad. After thermal treatment at 623 K, only the bands within 1360–1470 and 1500–1600 cm^{-1} (C=O) and shoulder at 1254 cm^{-1} (C–O) are observed in IR spectrum (Fig. 2b, 623 K). The experimentally observed 58% weight loss at 623 K is very close to the theoretically calculated 59% value which corresponds to the formation of manganese carbonate species (Scheme 1). The final 72% weight loss is observed after thermal treatment at 650 K. The bands within 1500–1600 and 1700–1800 cm^{-1} (C=O) are present in IR spectrum after $\text{Mn}(\text{acac})_3$ decomposition at 673 K (Fig. 2b, 673 K). The experimentally observed 72% weight loss at 650 K corresponds to the theoretically calculated 71% value and could be attributed to the formation of manganese oxy-carbonate species (Scheme 1).

The thermal decomposition of the supported $\text{Mn}(\text{acac})_3$ (Fig. 3a–d) differs from its bulk counterpart (Fig. 2a). The broad curves of the weight loss originated from superposition of the peaks are obvious for the $\text{Mn}(\text{acac})_3/\text{Al}_2\text{O}_3$ samples in contrast to narrow well-defined peaks of bulk $\text{Mn}(\text{acac})_3$.

A slight weight loss around 360 K is observed for all $\text{Mn}(\text{acac})_3/\text{Al}_2\text{O}_3$ samples and is absent in the case of bulk $\text{Mn}(\text{acac})_3$. This weight loss does not depend on $\text{Mn}(\text{acac})_3$ loading. Besides, the thermal treatment of $\text{Mn}(\text{acac})_3/\text{Al}_2\text{O}_3$ samples at 373 K does not lead to noticeable changes in IR spectrum (see, for example, Fig. 4). Therefore, one can attribute the observed weight loss to the removal of water adsorbed on the samples upon their storage in contact with air.

For $\text{Mn}(\text{acac})_3/\text{Al}_2\text{O}_3$ sample with 3.5 $\text{Mn}(\text{acac})_3/\text{nm}^2$ loading (Fig. 3a), the position of the maximum weight loss (600–650 K) coincides with the position of the corresponding high-temperature peak of bulk $\text{Mn}(\text{acac})_3$. Furthermore, this peak shows a distinct asymmetry similar to that observed in the case of bulk $\text{Mn}(\text{acac})_3$ (Fig. 2a). This confirms the presence of supported bulk-like $\text{Mn}(\text{acac})_3$ species in this sample and agrees with the results of its characterisation by IR spectroscopy (Fig. 1).

The position of the maximum weight loss, which occurs in the temperature interval 550–720 K in $\text{Mn}(\text{acac})_3/\text{Al}_2\text{O}_3$ samples, depends on $\text{Mn}(\text{acac})_3$ loading. One can see that decreasing of $\text{Mn}(\text{acac})_3$ loading results in the shift of the maximum to higher temperatures (Fig. 3a–d). For $\text{Mn}(\text{acac})_3/\text{Al}_2\text{O}_3$ samples with $\text{Mn}(\text{acac})_3$ loading of 3.5, 1.38, 0.74 and 0.35 $\text{Mn}(\text{acac})_3/\text{nm}^2$, the maximum of the weight loss are observed at 610, 620, 645 and 670 K, correspondingly. Most likely this is connected with high dispersion of surface bound $\text{Mn}(\text{acac})_{3-x}$

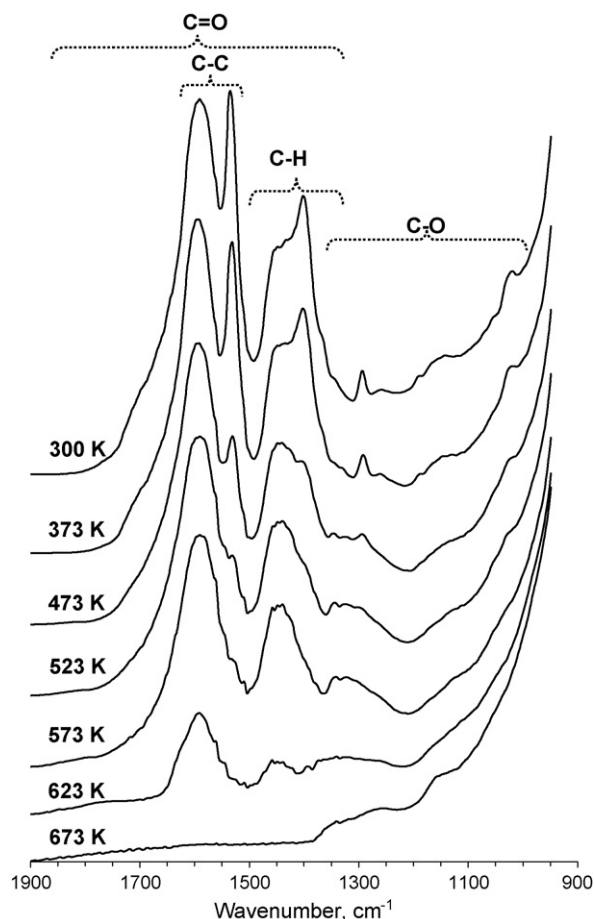


Fig. 4. Thermal decomposition of $\text{Mn}(\text{acac})_3/\text{Al}_2\text{O}_3$ sample with 0.74 $\text{Mn}(\text{acac})_3/\text{nm}^2$ loading: FTIR spectra after thermal treatment at different temperatures.

species which were observed in IR spectra at loading below 1.38 $\text{Mn}(\text{acac})_3/\text{nm}^2$ (Fig. 1). The role of surface $\text{Al}(\text{acac})_{3-x}$ species has to be also taken into account since decoration of the alumina surface with $\text{Mn}(\text{acac})_3$ is accompanied by their formation as was shown earlier. As $\text{Al}(\text{acac})_3$ is more thermally stable in comparison with $\text{Mn}(\text{acac})_3$ it is reasonable to assume that elimination of acetylacetonate ligands from surface $\text{Al}(\text{acac})_{3-x}$ species should occur at higher temperature as compared with surface $\text{Mn}(\text{acac})_{3-x}$ species.

IR studies show that in the case of the $\text{Mn}(\text{acac})_3/\text{Al}_2\text{O}_3$ sample with $\text{Mn}(\text{acac})_3$ loading of 0.74 $\text{Mn}(\text{acac})_3/\text{nm}^2$, the presence of supported bulk-like $\text{Mn}(\text{acac})_3$ species is not observed. Therefore, this sample was selected for the detailed investigation of thermal transformations of surface bound $\text{Mn}(\text{acac})_{3-x}$ species by IR spectroscopy and thermal analysis. Unfortunately, the quantitative interpretation of the obtained thermogravimetric data is complicated since the amount of acetylacetonate ligands which are present in the samples after drying can hardly be determined.

The weight loss within 425–550 K (Fig. 3c) is accompanied with the decreasing of intensity of the bands at 1535 (C–C), 1402 (C–H in CH_3), 1292 (C–O in C–O–Al) and 1255 cm^{-1} (C–O in C–O–Mn) in IR spectra (Fig. 4, 473 and 523 K). The weight loss

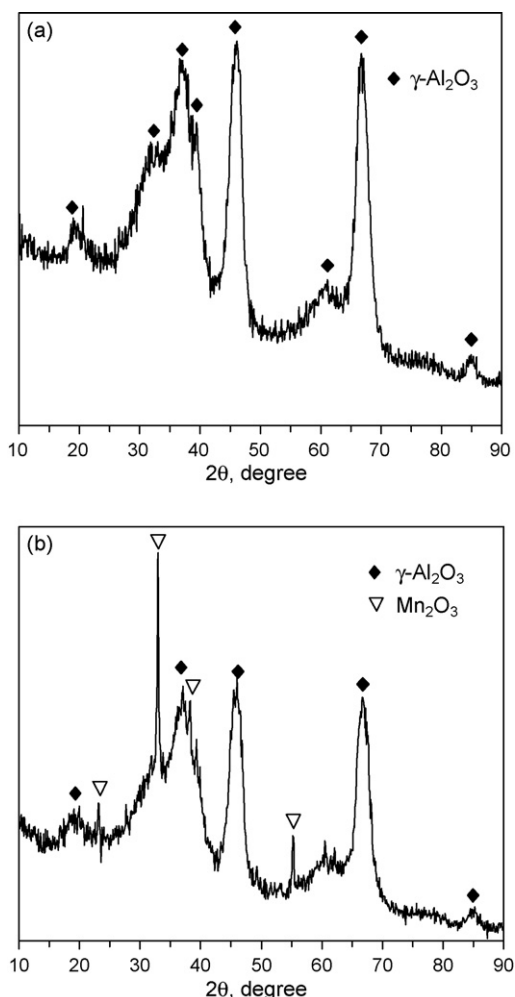


Fig. 5. XRD patterns of $\text{Mn}(\text{acac})_3/\text{Al}_2\text{O}_3$ samples after calcination at 873 K in air: (a) $0.74 \text{ Mn}(\text{acac})_3/\text{nm}^2$ loading and (b) $3.63 \text{ Mn}(\text{acac})_3/\text{nm}^2$ loading.

should be attributed to elimination of acetylacetonate ligands and partial oxidation of the remaining ligands without destruction of their cyclic structure like in the case of thermolysis of bulk $\text{Mn}(\text{acac})_3$. The main weight loss of the $\text{Mn}(\text{acac})_3/\text{Al}_2\text{O}_3$ sample takes place within 600–700 K and is caused by oxidative destruction of acetylacetonate ligands. Only the bands at $1225\text{--}1350 \text{ cm}^{-1}$ (C–O), $1400\text{--}1500$ and $1550\text{--}1650 \text{ cm}^{-1}$ (C=O) of carbonate and oxy-carbonate species are present in IR spectra after treatment at 573 and 623 K. All bands completely disappeared after treatment at 673 K that means a complete oxidative destruction of surface bound $\text{Mn}(\text{acac})_{3-x}$ species and their transformation into to manganese oxide species.

The dispersion of manganese oxide species on the alumina surface after thermal treatment of $\text{Mn}(\text{acac})_3/\text{Al}_2\text{O}_3$ samples at 873 K in air were evaluated by XRD. The calcined $\text{Mn}(\text{acac})_3/\text{Al}_2\text{O}_3$ sample with $\text{Mn}(\text{acac})_3$ loading of $0.74 \text{ Mn}(\text{acac})_3/\text{nm}^2$ exhibits high dispersion of the surface manganese oxide species since only XRD patterns of the initial $\gamma\text{-Al}_2\text{O}_3$ support are observed (Fig. 5a). In contrast, $\text{Mn}(\text{acac})_3/\text{Al}_2\text{O}_3$ sample with $\text{Mn}(\text{acac})_3$ loading of $3.63 \text{ Mn}(\text{acac})_3/\text{nm}^2$ (Fig. 5b) shows very intense and distinct XRD patterns confirming the presence of crystalline Mn_2O_3

(31-825 PDF). One can suppose that the dispersed surface manganese oxide species originate upon the oxidative thermolysis of the surface bound $\text{Mn}(\text{acac})_{3-x}$ species while crystalline Mn_2O_3 phase results from the supported bulk-like $\text{Mn}(\text{acac})_3$ species.

4. Conclusions

Decoration of $\gamma\text{-Al}_2\text{O}_3$ support with toluene solution of $\text{Mn}(\text{acac})_3$ results in the formation of surface bound $\text{Mn}(\text{acac})_{3-x}$ species when $\text{Mn}(\text{acac})_3$ loading does not exceed $1.38 \text{ Mn}(\text{acac})_3/\text{nm}^2$. At higher $\text{Mn}(\text{acac})_3$ loading the formation of the supported bulk-like $\text{Mn}(\text{acac})_3$ species also occurs. The interaction of $\text{Mn}(\text{acac})_3$ molecules with the support surface occurs via substitution of acetylacetonate ligand(s) with the oxygen atom of surface hydroxyl group(s) accompanied by elimination of acetylacetonate molecules. The evolved acetylacetonate reacts with the alumina surface that results in the formation of surface $\text{Al}(\text{acac})_{3-x}$ species.

Decomposition of bulk $\text{Mn}(\text{acac})_3$ takes place within 450–650 K and proceeds via oxidative destruction of acetylacetonate ligands and results in the formation of manganese oxy-carbonate species. Within 425–623 K, the elimination of one acetylacetonate ligand occurs. The remaining acetylacetonate ligands undergo the process of partial oxidation without destruction of their cyclic structure. Above 623 K, the oxidative destruction of the ligands occurs that results in the formation of manganese oxy-carbonate species.

The oxidative thermolysis of $\text{Mn}(\text{acac})_{3-x}$ species on the surface of γ -alumina proceeds via partial elimination of acetylacetonate ligands and partial oxidation of the remaining ligands without destruction of their cyclic structure within 425–550 K. The complete oxidative destruction of acetylacetonate ligands takes place within 600–700 K and results in formation of manganese oxide species on the alumina surface. The dispersed surface manganese oxide species originate upon the oxidative thermolysis of the surface bound $\text{Mn}(\text{acac})_{3-x}$ species while crystalline Mn_2O_3 phase results from the supported bulk-like $\text{Mn}(\text{acac})_3$ species.

Acknowledgement

This work was financially supported in part by the Commission of the European Communities in the frame of the INTAS 00-00413 and INCO-COPERNICUS ICA2-CT-2000-10021 projects.

References

- [1] W.R. Moser, *Advanced Catalysts and Nanostructured Materials*, Academic Press, San Diego, 1996.
- [2] J.C. Kevlin, M.G. White, M.B. Mitchell, Preparation and characterization of supported mononuclear metal complexes as model catalysts, *Langmuir* 7 (1991) 1198.
- [3] M. Baltes, P. Van Der Voort, B.M. Weckhuysen, R. Ramachandra Rao, G. Catana, R.A. Schoonheydt, E.F. Vansant, Synthesis and characterization of alumina-supported vanadium oxide catalysts prepared by the molecular designed dispersion of $\text{VO}(\text{acac})_2$ complexes, *Phys. Chem. Chem. Phys.* 2 (1992) 2673.

- [4] A. Hakuli, A. Kytokivi, Binding of chromium acetylacetonate on a silica support, *Phys. Chem. Chem. Phys.* 1 (1999) 1607.
- [5] O. Collart, P. Van Der Voort, E.F. Vansant, E. Gustin, A. Bouwen, D. Schoemaker, R. Ramachandra Rao, B.M. Weckhuysen, R.A. Schoonheydt, Spectroscopic characterization of an MoO₃ layer on the surface of silica. An evaluation of the molecular designed dispersion method, *Phys. Chem. Chem. Phys.* 1 (1999) 4099.
- [6] L.B. Backman, A. Rautiainen, A.O.I. Krause, M. Lindblad, A novel Co/SiO₂ catalysts for hydrogenation, *Catal. Today* 43 (1998) 11.
- [7] L.B. Backman, A. Rautiainen, M. Lindblad, A.O.I. Krause, Effect of support and calcination on the properties of cobalt catalysts prepared by gas phase deposition, *Appl. Catal. A: Gen.* 191 (2000) 55.
- [8] R. Molina, M.A. Centeno, G. Poncelet, α -Alumina-supported nickel catalysts prepared with nickel acetylacetonate. 1. Adsorption in the liquid phase, *J. Phys. Chem. B* 103 (1999) 6036.
- [9] R. Molina, G. Poncelet, α -Alumina-supported nickel catalysts prepared with nickel acetylacetonate. 2. A study of the thermolysis of the metal precursor, *J. Phys. Chem. B* 103 (1999) 11290.
- [10] J. Villasenor, P. Reyes, G. Pecchi, Catalytic and photocatalytic ozonation of phenol on MnO₂ supported catalysts, *Catal. Today* 76 (2002) 121.
- [11] T.-Ke Tseng, Chu Hsin, H.-H. Hsu, Characterization of γ -alumina-supported manganese oxide as an incineration catalyst for trichloroethylene, *Environ. Sci. Technol.* 37 (2003) 171.
- [12] M.I. Zaki, M.A. Hasan, L. Pasupulety, N.E. Fouad, H. Knözinger, CO and total oxidation over manganese CH₄ oxide supported on ZrO₂, TiO₂, TiO₂-Al₂O₃ and SiO₂-Al₂O₃ catalysts, *New J. Chem.* 23 (1999) 23.
- [13] Y. Liu, M. Luo, Z. Wei, Q. Xin, P. Ying, C. Li, Catalytic oxidation of chlorobenzene on supported manganese oxide catalysts, *Appl. Catal. B* 29 (2001) 61.
- [14] P. Fabrizioli, T. Bürgi, A. Baiker, Manganese oxide-silica aerogels: synthesis and structural and catalytic properties in the selective oxidation of NH₃, *J. Catal.* 207 (2002) 88.
- [15] J.I. Gutierrez-Ortiz, R. Lopez-Fonseca, U. Aurrekoetxea, J.R. Gonzalez-Velasco, Low-temperature deep oxidation of dichloromethane and trichloroethylene by H-ZSM-5-supported manganese oxide catalysts, *J. Catal.* 218 (2003) 148.
- [16] C. Reed, Y.-K. Lee, S. Ted Oyama, Structure and oxidation state of silica-supported manganese oxide catalysts and reactivity for acetone oxidation with ozone, *J. Phys. Chem. B* 110 (2006) 4207.
- [17] F. Kapteijn, A.D. Van Langeveld, J.A. Moulijn, A. Andrei, M.A. Vuurman, A.M. Turek, J.M. Jehng, I.E. Wachs, Alumina-supported manganese oxide catalysts. I. Characterization: effect of precursor and loading, *J. Catal.* 150 (1994) 94.
- [18] A.J. Renouprez, J.F. Trillat, B. Moraweck, J. Massardier, G. Bergeret, Pd-Mn silica supported catalysts. 1. Formation of the bimetallic particles, *J. Catal.* 179 (1998) 390.
- [19] M.A. Vicente, C. Belver, R. Trujillano, V. Rives, A.C. Alvarez, J.-F. Lambert, S.A. Korili, L.M. Gandia, A. Gil, Preparation and characterization of Mn- and Co-supported catalysts derived from Al-pillared clays and Mn- and Co-complexes, *Appl. Catal. A* 267 (2004) 47.
- [20] J.Y.H. Chau, P. Hanprasopwattana, Infrared solvent shift studies. I. Acetylacetonates of some trivalent transition metals, *Aust. J. Chem.* 28 (1975) 1689.
- [21] K. Nakamoto, *Infrared and Raman Spectra of Inorganic and Coordination Compounds*, third ed., Wiley, New York, 1978.
- [22] J.A.R. Van Veen, G. Jonkers, W.H. Hesselink, Interaction of transition-metal acetylacetonates with γ -Al₂O₃ surfaces, *J. Chem. Soc., Faraday Trans.* 85 (1989) 389.
- [23] S.M. Alexander, D.M. Bibby, R.F. Howe, R.H. Meinhold, Interaction of acetylacetonate with HZSM-5: visualization of “n.m.r. invisible” aluminum, *Zeolites* 13 (1993) 441.
- [24] A. Kytokivi, A. Rautiainen, A. Root, Reaction of acetylacetonate vapour with γ -alumina, *J. Chem. Soc., Faraday Trans.* 93 (1997) 4079.
- [25] I.C. McNeill, J.J. Ligat, The effect of metal acetylacetonates on the thermal degradation of poly(methylmethacrylate): part II—manganese (III) acetylacetonate, *Polym. Degrad. Stab.* 37 (1992) 25.